ISSN: 2633-4828 Vol. 5 No. S6, (Oct - Dec 2023)

International Journal of Applied Engineering & Technology

PARAMETRIC INVESTIGATION ON WELD CHARACTERISTICS FOR A SINGLE PASS TIG WELDED JOINT OF SS304

Vipul Patel, Rakesh Oza and Bhargav Patel
Assistant Professor, Mechanical Engineering Department, Government Engineering College Patan, Gujarat, India

ABSTRACT
Tungsten Inert Gas welding is one of the most popular methods for connecting ferrous and nonferrous metals. In this study, SS304 sheet materials with thicknesses of 1 mm and 3 mm were welded using TIG welding. The welding process parameters, specifically welding current and gas flow rate, were investigated for their impact on weld quality. The Taguchi method used an orthogonal array design to vary these factors across experiments systematically. ANOVA analysis was conducted to assess the significance of the control factors and to analyze their effects on weld pool geometry, specifically the front width and back width. The goal was to identify the optimal welding parameters that would result in the desired weld pool geometry. The analysis revealed that welding current emerged as the most significant control factor influencing both the front width and back width of the weld pool. Adjusting the welding current was therefore identified as critical for achieving the optimal weld pool geometry in this study.

1. INTRODUCTION
Ferrous and non-ferrous structures are widely utilized in virtually every global industry. These structural components are predominantly manufactured through processes like machining oversized ingots, superplastic forming, extrusion, or forging, which are expensive and lead to substantial scrap generation[1]. Among the different manufacturing methods, welding addresses this issue by first joining smaller workpieces together and then machining the component to the required dimensions. This approach significantly reduces the amount of material needed. Additionally, welded components exhibit similar quality and structural integrity, ensuring reliable, long-term functionality without failures[2]. At present, TIG welding stands out as a highly effective process for producing high-quality structural components with significant industrial potential[3].

Tungsten Inert Gas (TIG) welding, also referred to as Gas Tungsten Arc Welding (GTAW), has established itself as one of the most versatile and precise welding techniques in modern industry. Originating in the 1940s, TIG welding has profoundly impacted numerous sectors by providing exceptional control and high-quality metal joining capabilities. This introduction seeks to explore the foundational aspects of TIG welding, including its historical development, fundamental principles, extensive applications across various industries, and its crucial role in contemporary manufacturing processes[4], [5], [6]. Figure 1 shows the schematic diagram of the TIG welding process.

Stainless steel, or corrosion-resistant steel, constitutes a group of iron-based alloys renowned for their exceptional corrosion resistance. Due to this characteristic, stainless steel sheets are increasingly favored in applications such as kitchens, transportation, and building construction. Among the various types of stainless steel, austenitic steels are particularly esteemed for their blend of robust mechanical properties and superior corrosion resistance[7].

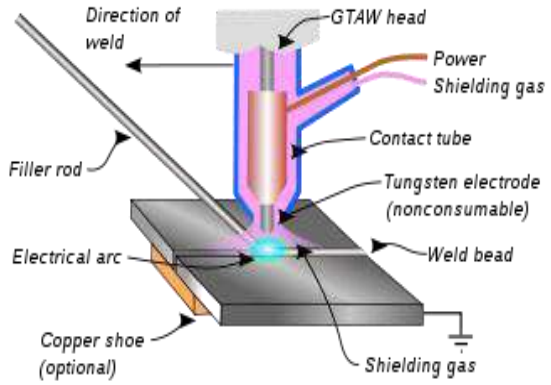

Fig.1 Tungsten Inert Gas Welding Process[8].

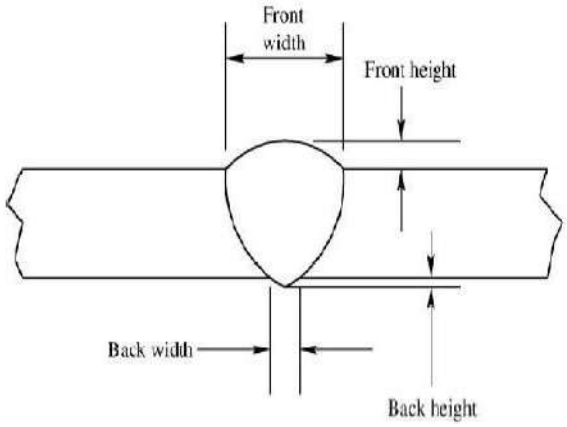

Fig. 2 Schematic diagram for weld bead geometry [9]

TIG welding was carried out of copper material. the process parameters that have been considered here are welding speed, wire feed rate, % cleaning, gap, and welding current. The effect of variation of these parameters has been considered on weld quality and optimal parameters have been suggested through experimental observations which consider the quality of the bead. TIG welding carried out on China low activation martensitic (CLAM) steel In this study, two plates of CLAM steel were butt-welded by TIG under identical conditions and archived hardening at the weld metal zone and softening in Heat affected zone[4]. Xiaodong Qi[10] researched how adding a Ni interlayer between Mg alloy and steel affects their joint interface. They found that compared to joints without any interlayer, the shear strength of the joint was notably enhanced. Ahmed Khalid Hussain[11] researched how welding speed influences the tensile strength of welded joints. His experiments focused on single V butt joints with varying bevel angles and heights. The findings showed that as the bevel height of the V butt joint increased, the depth of weld bead penetration decreased. The highest tensile strength observed was 230 MPa, achieved at a welding speed of 0.6 cm/sec, specifically with a 40º bevel angle and a 1.5 bevel height. LIU Xu-he[12] conducted TIG welding experiments on super-light magnesium-lithium alloy plates, each 2 mm thick, using argon gas as a protective atmosphere. The results revealed a fine microstructure in the fusion zone but a coarse one in the heat-affected zone (HAZ). It was observed that the HAZ is the weaker region of the weld plate. The tensile strength of the TIG welded plate was measured at 143.73 MPa, which corresponds to 84% of the strength of the parent metal. Fractures were predominantly located in the heat-affected zone, showing a mixed-mode fracture behavior characterized by a combination of ductile and brittle modes. S. C. Juang[13] researched to optimize process parameters for achieving optimal weld pool geometry in tungsten inert gas (TIG) welding of stainless steel. The experimental results demonstrated significant improvements in the front height, front width, back height, and back width of the weld pool by employing this approach.

Fig. 2 illustrates the geometric parameters of the bead in the TIG welding process. These parameters, such as bead width, bead height, penetration depth, and others, play a crucial role in determining the mechanical properties of the weld bead. The geometric characteristics of the bead are directly influenced by the input process parameters of the welding operation. Therefore, optimizing these process parameters can significantly impact the final mechanical properties of the welded joint, including strength, ductility, and toughness. Understanding and controlling these geometric parameters through proper selection and adjustment of welding parameters are essential steps in achieving high-quality welds with desired mechanical properties.

From the literature review, it is evident that while many researchers have studied various parameters and components of the welding process, there remains a significant gap in the clear definition of process parameter optimization. So, I have attempted to define objectives by systematically investigating various parameters of the TIG welding process to optimize its efficiency and effectiveness.

2. MATERIAL AND METHODS:

In this study, Stainless Steel (SS) 304 alloy plates of dimensions 25x100 mm with thicknesses of 1 mm and 3 mm were used, a total of 32 pieces. Properties of base metal are listed in Table 1. TIG welding experiments were conducted, with 16 experiments performed for each thickness of the plate. The key process parameters investigated were plate thickness, welding current, and gas flow rate. Before welding, the SS304 plates underwent surface cleaning and proper finishing of all four edges to ensure a clean and uniform welding surface. Chamfering was also performed, with a chamfer depth ranging from 2 to 4 mm, to enhance weld penetration. The welding itself was conducted using a TIG apparatus, following the specified parameters. To systematically analyze the effects of these parameters on weld quality, an L16 orthogonal array was employed as part of the Taguchi method for design of experiments. This approach allows for efficient testing and optimization of welding parameters to achieve desired weld pool characteristics and overall welding performance. Travelling microscope were measure the width and length of weld pool.

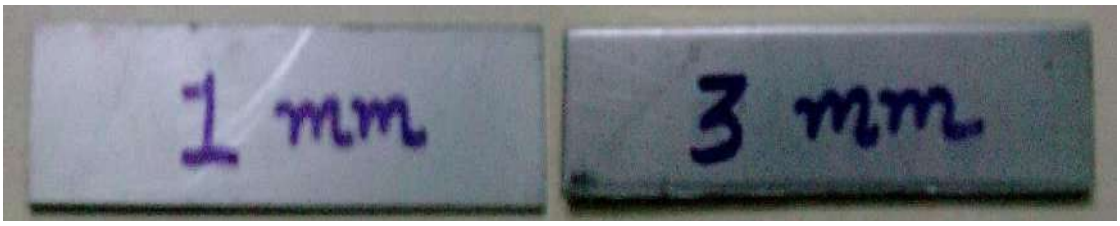

Figure 3: Workpiece material SS304.

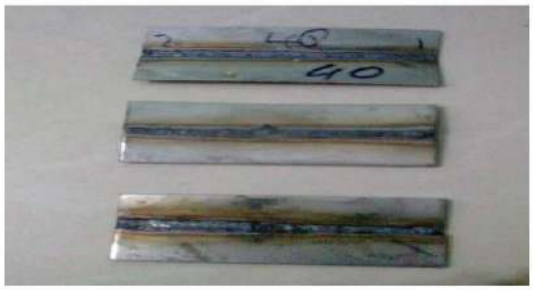

Figure 4: Welded job

Table 1: Properties of SS304 plate.

Chemical Properties				Mechanical Properties			
%C	%Cr	%Ni	%Mo	Tensile strength	Poisson's ratio	Shear modulus	Modulus of elasticity
0.070	18.450	8.100	0.250	505 Mpa	0.29	86 Gpa	193-200Gpa

3. DESIGN OF EXPERIMENT:

Dr. Taguchi, associated with Nippon Telephones and Telegraph Company in Japan, pioneered a method based on orthogonal array experiments. This approach significantly reduces experimental variance by systematically varying control parameters in a structured way. The Taguchi Method involves the Design of Experiments (DOE) aimed at optimizing these control parameters to achieve the best possible results. Orthogonal arrays are specifically designed matrices that allow for a minimal number of experiments while ensuring balanced coverage of parameter combinations. Dr. Taguchi's method employs Signal-to-Noise ratios (S/N ratios), which are logarithmic functions of desired output characteristics. These S/N ratios serve as objective functions during optimization, aiding in the analysis of experimental data and prediction of optimal settings for control parameters. Overall, the Taguchi Method is widely recognized for its efficiency in experimental design, robustness in

optimization, and its ability to provide actionable insights into improving processes and products through systematic experimentation.

In the present experimental work, an L16 Taguchi standard orthogonal array was selected for the design of experiments. Since the number of factors is two with four levels, therefore the most suitable Taguchi orthogonal array for the experiment was the L16 array as shown in Table 2. Since this is a main effects array, the interactions among the factors are spread more or less equally among the columns; the method pushes quality back to the design stage, seeking to design a product/process, that is insensitive to quality problems.

Table 2: Process Parameters Levels:

Thickness (mm)	Process Parameters	Level 1	Level 2	Level 3	Level 4
1mm	Welding current (A)	30	40	50	60
	Gas flow rate (LPM)	1	2	3	4
3mm	Welding current (A)	80	110	120	140
	Gas flow rate (LPM)	1.5	3.5	5.5	7.5

Table 3: L16 Orthogonal array in coded design

Exp No.	Welding current I (A)	Gas flow rate G (LPM)	1 mm plate thickness		3 mm plate thickness	
			FW (mm)	BW (mm)	FW (mm)	BW (mm)
1	1	1	4.100	3.15	5.400	3.920
2	1	2	3.570	3.28	5.420	4.020
3	1	3	3.930	3.12	5.920	4.200
4	1	4	3.530	3.15	6.500	4.000
5	2	1	4.190	3.60	6.460	5.210
6	2	2	4.048	3.54	5.920	5.480
7	2	3	4.060	4.01	6.270	5.760
8	2	4	4.200	3.90	7.010	4.510
9	3	1	4.860	3.98	7.100	5.150
10	3	2	4.600	4.10	7.390	5.700
11	3	3	4.200	4.00	7.050	5.700
12	3	4	4.530	4.05	7.880	5.020
13	4	1	4.950	4.42	7.871	5.550
14	4	2	4.810	4.40	8.580	5.820
15	4	3	4.850	4.02	8.010	6.290
16	4	4	4.700	3.89	8.120	6.082

4. RESULT AND DISCUSSION

4.1 Non Linear Regression Model for Front Width of 1 Mm and 3 Mm Thickness

Table 4: Estimated Regression Coefficients for Front width of 1 mm

Term	Coef	SE Coef	T	P
Constant	3.0028	0.970076	3.095	0.011
Welding Current	0.04831	0.040626	1.189	0.262
Gas flow rate	-0.41716	0.273058	-1.528	0.158
Welding Current*Welding Current	-0.00016	0.000439	-0.353	0.731
Gas flow rate*Gas flow rate	0.062	0.043859	1.414	0.188

Welding Current*Gas flow rate	0.00049	0.003509	0.139	0.892
S = 0.175437 PRESS = 0.901784 R-Sq = 89.91% R-Sq(pred) = 70.44% R-Sq(adj) = 84.87%				

Table 5: Analysis of Variance for Front width of 1 mm

Source	DF	Seq SS	Adj SS	Adj MS	F
Regression	5	2.743	2.743	0.548599	17.82
Linear	2	2.67705	0.13137	0.065684	2.13
Welding Current	1	2.53187	0.04352	0.043522	1.41
Gas flow rate	1	0.14518	0.07184	0.071836	2.33
Square	2	0.06535	0.06535	0.032674	1.06
Welding Current*Welding Current	1	0.00384	0.00384	0.003844	0.12
Gas flow rate*Gas flow rate	1	0.0615	0.0615	0.061504	2
Interaction	1	0.0006	0.0006	0.000595	0.02
Welding Current*Gas flow rate	1	0.0006	0.0006	0.000595	0.02
Residual Error	10	0.30778	0.30778	0.030778	
Total	15	3.05078			

Regression equation for 1 mm Front Width.

$$FW = 3.0028 + 0.04831 \times I - 0.41716 \times G - 0.00016 \times I \times I + 0.062 \times G \times G + 0.00049 \times I \times G$$

The unknown coefficients are computed using the experimental data that are displayed in Tables 4 and 6. A tabulation of the standard errors on the coefficient estimations may be seen in the "SE coef" column. The following is the formulation of the front width of nonlinear regression equations. The significance of how much of the variation in the response is described by the model is shown by the coefficient of determination (R^2), which is at 89.91% and 90.88% for Fornt width of 1 mm and 3 mm respectively. A higher R2 value suggests that the model fits the data more accurately.

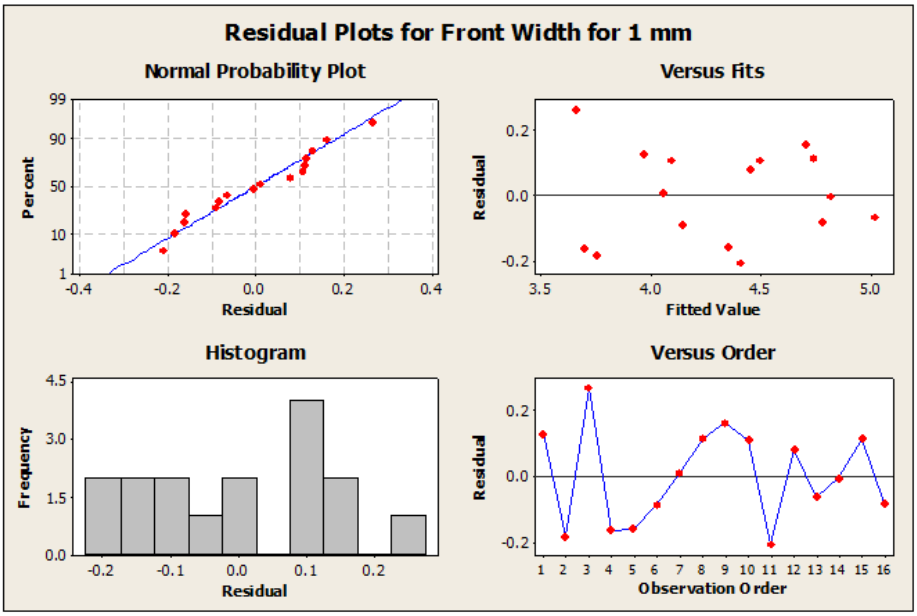

Figure 5: Residual plot for Front width of 1 mm thickness

Table 6: Estimated Regression Coefficients for Front width of 3 mm				
Term	**Coef**	**SE Coef**	**T**	**P**
Constant	6.5102	0.1807	36.025	0
Welding Current	1.2116	0.1282	9.452	0
Gas flow rate	0.3209	0.1243	2.581	0.027
Welding Current*Welding Current	0.3429	0.1952	1.756	0.11
Gas flow rate*Gas flow rate	0.2505	0.2071	1.209	0.254
Welding Current*Gas flow rate	-0.2607	0.1711	-1.524	0.159

S = 0.368128 PRESS = 3.51419

R-Sq = 90.88% R-Sq(pred) = 76.35% R-Sq(adj) = 86.32%

It is important to check the adequacy of the fitted model, because an incorrect or under-specified model can lead to misleading conclusions. By checking the fit of the model one can check whether the model is under specified. The Analysis of variance for Fornt width of 1 mm and 3 mm were calculated based on 95% confidence level depicted in Table no. 5 and 7.

Regression equation for 3 mm Front Width.

$$FW = 6.5102 + 1.2116 \times I + 0.3209 \times G + 0.3429 \times I \times I + 0.2505 \times G \times G - 0.2607 \times I \times G$$

Table 7: Analysis of Variance for Front width of 3 mm					
Source	**DF**	**Seq SS**	**Adj SS**	**Adj MS**	**F**
Regression	5	13.5017	13.5017	2.7003	19.93
Linear	2	12.5707	13.0095	6.5048	48
Welding Current	1	11.7753	12.1064	12.1064	89.33
Gas flow rate	1	0.7954	0.9031	0.9031	6.66
Square	2	0.6163	0.6163	0.3082	2.27
Welding Current*Welding Current	1	0.4181	0.4181	0.4181	3.08
Gas flow rate*Gas flow rate	1	0.1982	0.1982	0.1982	1.46
Interaction	1	0.3147	0.3147	0.3147	2.32
Welding current*Gas flow rate	1	0.3147	0.3147	0.3147	2.32
Residual Error	10	1.3552	1.3552	0.1355	
Total	15	14.8569			

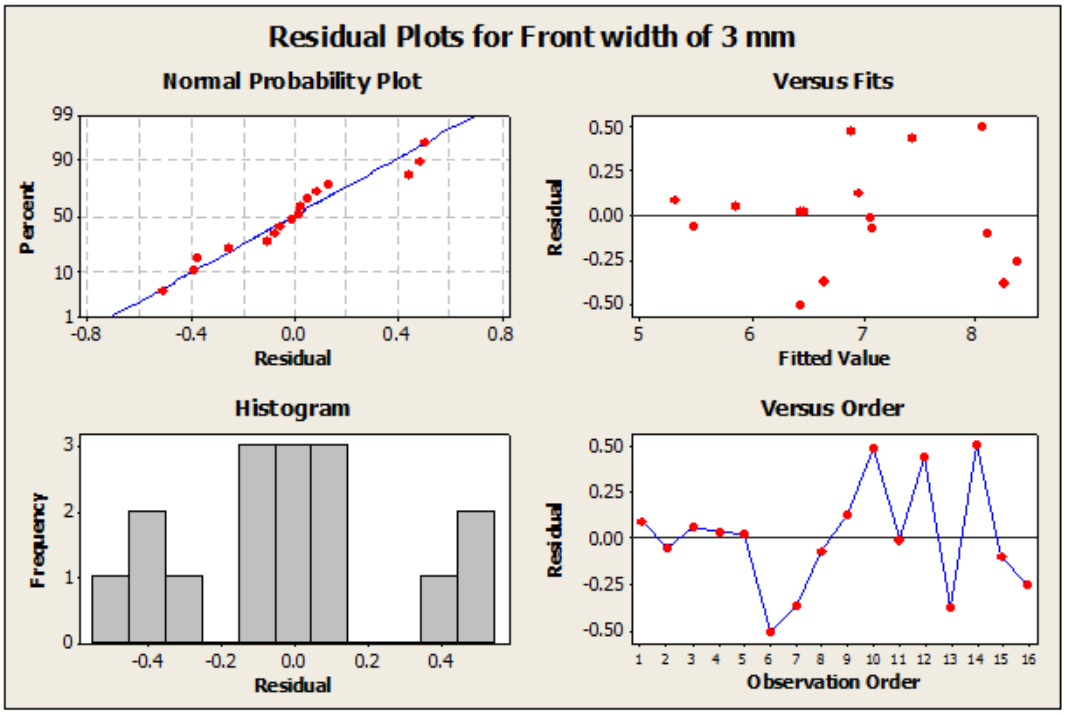

Figure 6: Residual plot for Front width of 3 mm thickness

The residual plot of front width for 1mm and 3 mm is shown in figure 5 and 6. This layout is useful to determine whether the model meets the assumptions of the analysis or not. Normal probability plot indicates the data are normally distributed and the variables are influencing the response. Outliers don't exist in the data, because standardized residues are between -1 and 1.

4.2 Non Linear Regression Model for Back Width of 1 Mm and 3 Mm Thickness

The unknown coefficients are computed using the experimental data that are displayed in Tables 8 and 10. The following is the formulation of the back width of nonlinear regression equations. The significance of how much of the variation in the response is described by the model is shown by the coefficient of determination (R^2), which is at 89.88% and 91.33% for Back width of 1 mm and 3 mm respectively.

Table: 8 Estimated Regression Coefficients for Back width of 1 mm

Term	Coef	SE Coef	T	P
Constant	-0.58675	0.92451	-0.635	0.54
Welding Current	0.148088	0.038718	3.825	0.003
Gas flow rate	0.387925	0.260232	1.491	0.167
Welding Current*Welding Current	-0.00109	0.000418	-2.617	0.026
Gas flow rate*Gas flow rate	-0.02063	0.041799	-0.493	0.632
Welding current*Gas flow rate	-0.00669	0.003344	-2.001	0.073
S = 0.167197 PRESS = 0.781395				
R-Sq = 89.88% R-Sq(pred) = 71.72% R-Sq(adj) = 84.82%				

Table: 9 Analysis of Variance for Back width of 1 mm

Source	DF	Seq SS	Adj SS	Adj MS	F
Regression	5	2.4835	2.4835	0.496699	17.77
Linear	2	2.17339	0.4381	0.21905	7.84
Welding Current	1	2.16811	0.40895	0.408949	14.63

Gas flow rate	1	0.00528	0.06212	0.06212	2.22
Square	2	0.19821	0.19821	0.099106	3.55
Welding Current*Welding Current	1	0.19141	0.19141	0.191406	6.85
Gas flow rate*Gas flow rate	1	0.00681	0.00681	0.006806	0.24
Interaction	1	0.11189	0.11189	0.11189	4
Welding Current*Gas flow rate	1	0.11189	0.11189	0.11189	4
Residual Error	10	0.27955	0.27955	0.027955	
Total	15	2.76304			

Regression equation for 1 mm Back Width.

$$BW = -0.58675 + 0.14808 \times I + 0.38792 \times G - 0.00109 \times I \times I - 0.02063 \times G \times G - 0.00669 \times I \times G$$

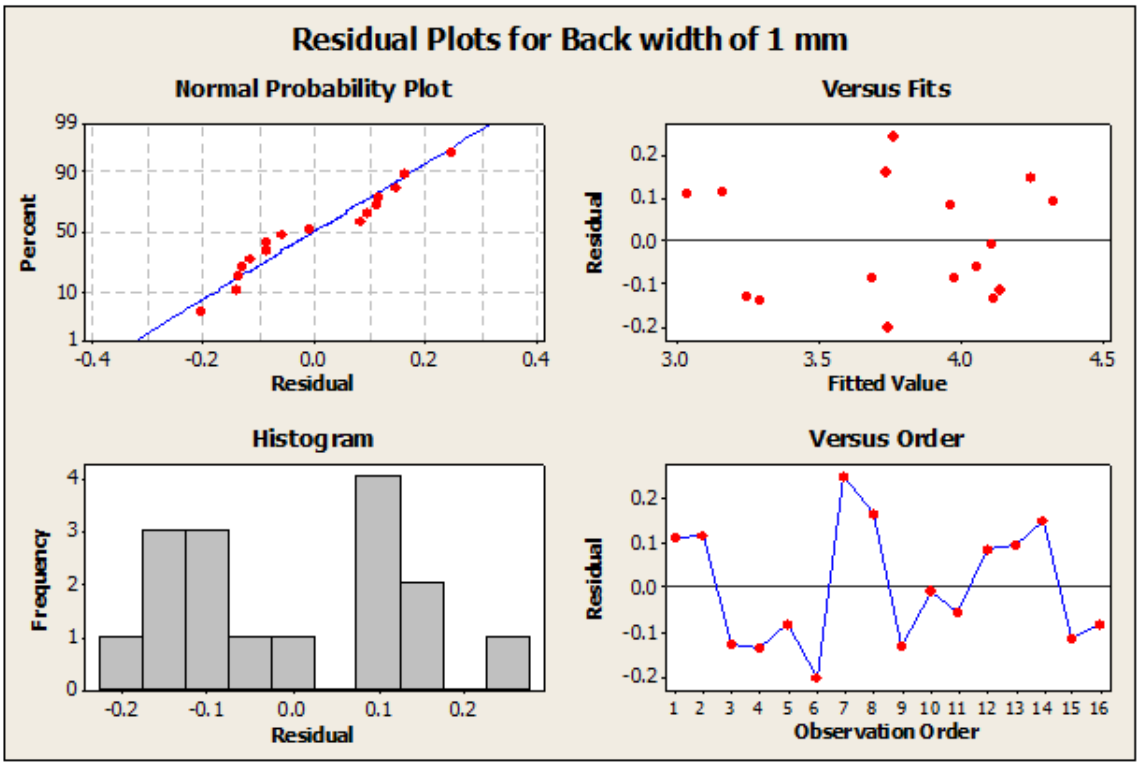

Figure 7: Residual plot for Back width of 1 mm thickness

Table: 10 Estimated Regression Coefficients for Back width of 3 mm

Term	Coef	SE Coef	T	P
Constant	5.45037	0.13946	39.083	0
Welding Current	0.93802	0.09892	9.483	0
Gas flow rate	0.00139	0.09592	0.015	0.989
Welding Current*Welding Current	-0.19358	0.15066	-1.285	0.228
Gas flow rate*Gas flow rate	-0.49613	0.15979	-3.105	0.011
Welding current*Gas flow rate	0.1075	0.13203	0.814	0.434

S = 0.284078 PRESS = 2.60206

R-Sq = 91.33% R-Sq(pred) = 72.04% R-Sq(adj) = 87.00%

Table: 11 Analysis of Variance for Back width of 3 mm

Source	DF	Seq SS	Adj SS	Adj MS	F
Regression	5	8.50101	8.50101	1.7002	21.07
Linear	2	7.53636	7.25669	3.62835	44.96
Welding Current	1	7.53541	7.25668	7.25668	89.92
Gas flow rate	1	0.00095	0.00002	0.00002	0
Square	2	0.91116	0.91116	0.45558	5.65
Welding Current*Welding Current	1	0.13323	0.13323	0.13323	1.65
Gas flow rate*Gas flow rate	1	0.77792	0.77792	0.77792	9.64
Interaction	1	0.0535	0.0535	0.0535	0.66
Welding Current*Gas flow rate	1	0.0535	0.0535	0.0535	0.66
Residual Error	10	0.807	0.807	0.0807	
Total	15	9.30802			

Regression equation for 3 mm Back Width.

$$BW = 5.45037 + 0.93802 \times I + 0.00139 \times G - 0.19358 \times I \times I - 0.49613 \times G \times G + 0.1075 \times I \times G$$

It is important to check the adequacy of the fitted model, because an incorrect or under-specified model can lead to misleading conclusions. By checking the fit of the model one can check whether the model is under specified. The Analysis of variance for Back width of 1 mm and 3 mm were calculated based on 95% confidence level depicted in Table no. 9 and 11.

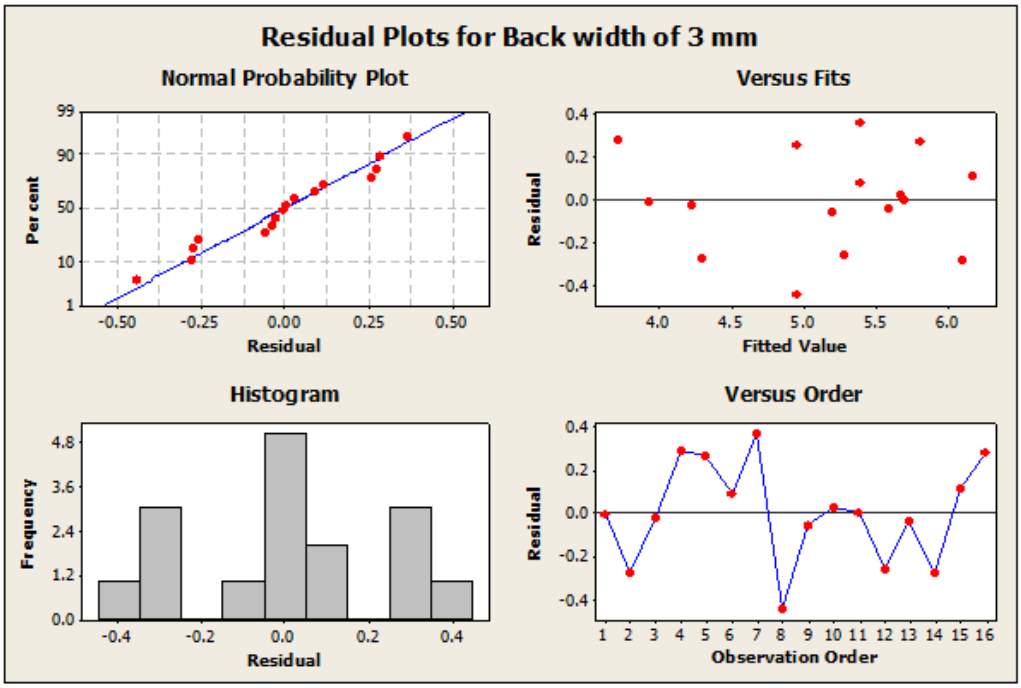

Figure 8: Residual plot for Back width of 3 mm thickness

The residual plot of Back width for 1 mm and 3 mm is shown in figure 7 and 8. This layout is useful to determine whether the model meets the assumptions of the analysis or not. Residuals versus fitted values indicate the variance is constant and a nonlinear relationship exists as well as no outliers exist in data. Histogram proves the data are not skewed and not outliers exist.

5. CONCLUSION

In present study parametric analysis has been carried out for front width and back width on SS304 material. Experiments are carried out using L16 Orthogonal array by varying welding current and gas flow rate for different thickness of SS304 material.

- Whenever the gas flow rate is constant from 1 (LPM) to 4 (LPM) and welding current is increase from 30 (A) to 60 (A) at same time front width and back width both are increase for 1 mm thickness.
- Whenever the gas flow rate is constant from 1.5 (LPM) to 7.5 (LPM) and welding current is increase from 80 (A) to 140 (A) at same time front width and back width both are increase for 3 mm thickness.
- The minimum front width obtained is at welding current 30 (A) and gas flow rate 2 LPM and minimum back width obtained is at welding current 30 (A) and gas flow rate 4 LPM for 1 mm thickness.
- The minimum front width and back width obtained is at welding current 80 (A) and gas flow rate 1.5 LPM for 3 mm thickness.

REFERENCE

[1] S. N. Singh *et al.*, "A Comparative Analysis of Laser Additive Manufacturing of High Layer Thickness Pure Ti and Inconel 718 Alloy Materials Using Finite Element Method," *Materials*, vol. 14, no. 4, p. 876, Feb. 2021, doi: 10.3390/ma14040876.

[2] A. K. Singh, V. Dey, and R. N. Rai, "Techniques to improveweld penetration in TIG welding (A review)," *Mater Today Proc*, vol. 4, no. 2, pp. 1252–1259, 2017, doi: 10.1016/j.matpr.2017.01.145.

[3] K. Kumar, Ch. Sateesh Kumar, M. Masanta, and S. Pradhan, "A review on TIG welding technology variants and its effect on weld geometry," *Mater Today Proc*, vol. 50, pp. 999–1004, 2022, doi: 10.1016/j.matpr.2021.07.308.

[4] Q. Zhu, Y. Lei, X. Chen, W. Ren, X. Ju, and Y. Ye, "Microstructure and mechanical properties in TIG welding of CLAM steel," *Fusion Engineering and Design*, vol. 86, no. 4–5, pp. 407–411, Jun. 2011, doi: 10.1016/j.fusengdes.2011.03.070.

[5] A. K. Singh, V. Dey, and R. N. Rai, "Techniques to improveweld penetration in TIG welding (A review)," *Mater Today Proc*, vol. 4, no. 2, pp. 1252–1259, 2017, doi: 10.1016/j.matpr.2017.01.145.

[6] A. C. R. A.Balaram Naik, "Experimental Analysis of TIG Welding and Comparison between Activated-TIG and TIG on Duplex Stainless Steel (2205)," *International Journal of Scientific & Engineering Research ISSN 2229-5518*, vol. Volume 7, no. Issue 6, p. 115, Jun. 2016.

[7] W. Chuaiphan and L. Srijaroenpramong, "Effect of hydrogen in argon shielding gas for welding stainless steel grade SUS 201 by GTA welding process," *Journal of Advanced Joining Processes*, vol. 1, p. 100016, Mar. 2020, doi: 10.1016/j.jajp.2020.100016.

[8] R. Kumar, N. Ramesh Mevada, S. Rathore, N. Agarwal, V. Rajput, and A. S. Barad, "Experimental Investigation and Optimization of TIG Welding Parameters on Aluminum 6061 Alloy Using Firefly Algorithm," *IOP Conf Ser Mater Sci Eng*, vol. 225, p. 012153, Aug. 2017, doi: 10.1088/1757-899X/225/1/012153.

[9] P. Dutta and D. K. Pratihar, "Modeling of TIG welding process using conventional regression analysis and neural network-based approaches," *J Mater Process Technol*, vol. 184, no. 1–3, pp. 56–68, Apr. 2007, doi: 10.1016/j.jmatprotec.2006.11.004.

[10] X. Qi and G. Song, "Interfacial structure of the joints between magnesium alloy and mild steel with nickel as interlayer by hybrid laser-TIG welding," *Mater Des*, vol. 31, no. 1, pp. 605–609, Jan. 2010, doi: 10.1016/j.matdes.2009.06.043.

[11] A. L. M. J. Pramesh. T. Ahmed Khalid Hussain, "Influence of Welding Speed on Tensile Strength of Welded Joint in TIG Welding Process," *INTERNATIONAL JOURNAL OF APPLIED ENGINEERING RESEARCH, DINDIGUL*, vol. 1, no. 3, 2010.

[12] X. LIU, S. GU, R. WU, X. LENG, J. YAN, and M. ZHANG, "Microstructure and mechanical properties of Mg-Li alloy after TIG welding," *Transactions of Nonferrous Metals Society of China*, vol. 21, no. 3, pp. 477–481, Mar. 2011, doi: 10.1016/S1003-6326(11)60739-5.

[13] S. C. Juang and Y. S. Tarng, "Process parameter selection for optimizing the weld pool geometry in the tungsten inert gas welding of stainless steel," *J Mater Process Technol*, vol. 122, no. 1, pp. 33–37, Mar. 2002, doi: 10.1016/S0924-0136(02)00021-3.